SECOND HARMONIC GENERATION IN FERROELECTRIC $LiTaO_3$ AND $KNbO_3$ CONTAINING BULK NANO GLASS-CERAMICS

ANAL TARAFDER[a], KALYANDURG ANNAPURNA[a], REENAMONI SAIKIA CHALIHA[a], SRINIBAS SATAPATHY[b], VIDYA SAGAR TIWARI [b], PRADEEP KUMAR GUPTA[b] and BASUDEB KARMAKAR [a,*]

[a]*Glass Science & Technology Section, Glass Division, Central Glass and Ceramic Research Institute, Council of Scientific and Industrial Research (CSIR, India), 196, Raja S. C. Mullick Road, Kolkata 700 032, India*
[b]*Laser Materials Development and Devices Division, Raja Ramanna Center for Advanced Technology, Indore 452 013, India*

Abstract

The precursor glasses in (mol%) $25.53Li_2O$-$21.53Ta_2O_5$-$35.29SiO_2$-$17.65Al_2O_3$ (LTSA) and $25K_2O$-$25Nb_2O_5$-$50SiO_2$ (KNS) glass systems were prepared by the melt-quench technique. Ferroelectric $LiTaO_3$ (LT) and $KNbO_3$ (KN) crystallites containing bulk nano glass-ceramics have been prepared by controlled crystallization of these precursor glasses respectively. Second harmonic generations (SHG) at 532 nm in both the glass-ceramics have been realized under fundamental beam of Nd^{3+}:YAG laser source (1064 nm). The SHG power output has been found to increase up to 14 and 62.4 nJ with variation of rotation angle for LT and KN bulk nano glass-ceramics respectively due to orientation of ferroelectric domains under applied field.

Keywords: Glasses; bulk nano glass-ceramics; second harmonic generation.

[*]Corresponding author. Tel.: +91-33 2473 3469; fax: +91-33 2473 0957

E-mail address: basudebk@cgcri.res.in (B. Karmakar)

1. Introduction

The area of nonlinear optics (NLO) has gained considerable importance with the advent of lasers[1] and demonstration of second-harmonic generation (SHG) in a quartz crystal with an intense ruby laser beam by Franken and coworkers[2]. The generation of new output at different color with frequency twice that of ruby laser radiation has laid the foundations of nonlinear optics.[3,4] The electric field strength of conventional light sources is much lower as compared to the inter-atomic fields, and hence cannot demonstrate sizeable nonlinear effects. But the field strength of laser light is comparable to that of inter-atomic fields, so the nonlinear-optical effects are readily manifested.

NLO deals with the interaction of intense electromagnetic fields with matter, producing magnified fields that are different from the input field in frequency, phase or amplitude. NLO is essentially a material phenomenon, and the usual nonlinear medium is a crystal. Hence search for new nonlinear-optical materials with superior properties has got new momentum in the past few decades.

$LiTaO_3$ (LT) and $KNbO_3$ (KN) are the two most important lead-free ferroelectric materials in the $A^{1+}B^{5+}O_3$ type perovskite family. These materials exhibit excellent nonlinear optical properties in their single crystal forms.[5-8] Optical and structural properties of single crystal $LiTaO_3$ and $KNbO_3$ have also been studied due to their potential optical and optoelectronic applications.[9-14] In the last decade, significant interest has been articulated by the researcher in non-single crystal (vitreous, glass-ceramic and ceramic) optical media capable of producing optical second harmonic generation (SHG). The demands of optics and optoelectronics for fiber and waveguide materials with nonlinear properties have motivated the researchers to do so. However, the design of these glass materials has been basically hampered by the fact that glasses

have inversion symmetry and forbid the even-order optical nonlinearity, in particular, the SHG effect. This forbiddingness can be removed through a polar or noncentrosymmetric texturing of the material either owing to external actions or due to the formation and ordering of acentric internal fragments.[15-19]

Numerous publications during last several years are devoted to dc electrical poling of various glasses of complicated compositions such as potassium cesium niobium silicate[17], titanium silicate[18], lithium niobium tellurite[19], lead silicate[20], niobium borophosphate[21] and others. It should be emphasized that the SHG effect in poled glasses has exclusively electric-induced nature and does not involve noticeable atomic rearrangements on the scale of both short-range and medium-range orders. Therefore, SHG efficiency of poled glasses is not long living and may be easily suppressed by a subsequent low-temperature heat treatment[21] A brief review on optical nonlinearity in photonic glasses has been reported by Tanaka et al.[22] Electron beam induced SHG generation in Er^{3+} doped PbO-GeO_2 glasses containing silver nanoparticles has also been reported by Kassab et al.[23] In this connection, nanostructured glasses or transparent glass-ceramics based on ferroelectric or other highly polarizable phases are of great interest for different non-linear optical applications. At present, however, the nanometric scale is not sufficiently well mastered to allow manufacturing of nanostructured transparent glasses and glass ceramics possessing a distinct second order optical non-linearity. Recently, the structural and luminescence properties of rare earth doped $LiTaO_3$ and $KNbO_3$ glass-ceramics have been reported by our group[24,25] and other researchers[26] as well. However, as we aware distinct second order optical non-linearity in the volume nanocrystallized ferroelectric crystal of $LiTaO_3$ and $KNbO_3$ in bulk glass-ceramics has not been explored so far.

In view of above, the present work focuses on the preparation of $25.53Li_2O$-$21.53Ta_2O_5$-$35.29SiO_2$-$17.65Al_2O_3$ (LTSA) and $25K_2O$-$25Nb_2O_5$-$50SiO_2$ (KNS) precursor glasses and subsequently LT and KN nano glass-ceramics respectively, by controlled nucleation and crystallization processes. The consequences of crystallization have been studied by X-ray diffraction (XRD), transmission electron microscopy (TEM) and second harmonic generation (SHG) measurements.

2. Experimental

2.1 Precursor Glass Preparation

The precursor glass having molar composition (mol%) $25.53Li_2O$-$21.53Ta_2O_5$-$35.29SiO_2$-$17.65Al_2O_3$ and $25K_2O$-$25Nb_2O_5$-$50SiO_2$ were prepared from high-purity chemicals such as Li_2CO_3 (GR, 99%, Loba Chemie), K_2CO_3 (GR, 99.9%, Loba Chemie), Ta_2O_5 (99.85%, Alfa Aesar), Nb_2O_5 (GR, 99.9%, Loba Chemie), SiO_2 (99.8%, Sipur A1 Bremtheler Quartzitwerk) and Al_2O_3 (99.8%, CT 1200 SG, Almatis Inc.) by conventional melt-quench technique. The well-mixed batch of about 100 g of each glass was melted in a platinum crucible in an electric furnace at 1550-1600°C for 2 h in air. The glass melts were poured onto a pre-heated iron mould. They were annealed at 600°C for 4 h to remove the internal stresses of the glass and then slowly cooled down to room temperature. The as-prepared glass blocks were cut into desired dimensions and optically polished for ceramization and subsequently to perform SHG measurements.

2.2 Characterization

The crystalline phases generated in the glass matrices were identified by X-ray diffraction measurements using an X'Pert-Pro MPD diffractometer (PANalytical) with Ni-filtered CuK_α =

1.5406 Å radiation as the X-ray source. The 2θ scan range was 10^o to 80^o with a step size of 0.05^o. The TEM images and selected area electron diffraction (SAED) of powdered glass-ceramic samples were obtained using a Tecnai G^2 30ST transmission electron microscope (FEI Company).

SHG measurements were carried out using Nd: YAG laser (λ = 1064 nm) of pulse width 17 ns. The experimental set up for the measurement of relative second harmonic intensity is shown in Fig. 1. The input energy of Nd^{3+}: YAG laser was fixed at 17 mJ. The input energy of laser was divided in two directions (50% energy in each direction) using reflecting neutral density filter. In one direction KDP was put for reference. The reference SHG signal was measured using photodiode. Second beam was passed through visible filter (which blocks all visible wavelengths but pass 1064 nm) and focused onto the test samples. The SHG generated from the sample was focused onto a second harmonic separator, which reflects 532 nm at 45^o and transmit 1064 nm. The SHG signal reflected from SHG separator passed through IR filter was finally measured using PMT. The reference signals from photodiode and from PMT were measured simultaneously using Lecroy oscilloscope (bandwidth 1GHz).

3. Results and Discussion

3.1 X-ray Diffraction Analysis

The photographs of transparent precursor bulk LTSA and KNS glasses and their corresponding nano glass-ceramics (of different lengths) prepared by controlled crystallization of the precursor glasses at 680^oC for 10 h and 800^oC for 10 h respectively, and they are shown in Fig. 2(a) and (b) respectively. The X-ray diffractograms of precursor glass and cerammed glass-ceramics of both the systems are shown in Fig. 3 and Fig. 4. The XRD pattern of the precursor glasses exhibit

broad humps characterizing their amorphous nature. The X-ray diffraction pattern of the glass-ceramics in LTSA glass system clearly shows the structural behavior expected after a thermal treatment of the precursor glass. With increase of heat-treatment temperature, several diffraction peaks have been appeared. From the analysis of these peaks it has been concluded that these peaks are attributed to rhombohedral $LiTaO_3$ (JCPDS Card File No. 29-0836) except a few diffraction peak around $2\theta = 23.05^o$, 25.35^o, 44.60^o and 47.02^o which are due to the formation of β-spodumene ($LiAlSi_2O_6$) crystal phase (JCPDS Card File No. 35-0797) in minor quantity. It is clearly observed from the XRD analysis that the peak of $LiAlSi_2O_6$ ($2\theta = 25.27^o$) is more prominent in sample heat-treated at 680°C for 10 h duration and it got diminished with respect to $LiTaO_3$ phase in samples heat-treated at higher temperatures (here 750 and 850°C) for same duration of heat-treatment. This observation indicates that the β-spodumene content in glass-ceramics decreases with formation of more LT with increase in heat-treatment temperature. The structuring of broad hump in the $25K_2O$-$25Nb_2O_5$-$50SiO_2$ glass system takes place in the XRD pattern of the heat-treated nano glass-ceramic sample along with the appearance of other well defined peaks at around 15^o, 16^o, 25^o, 30^o, 51^o diffraction angles, which confirms the precipitation of crystalline phase in the amorphous matrix. The diffraction pattern of glass-ceramics to some extent resembles the JCPDS Card File No. 32-821 of known potassium niobate ($KNbO_3$) crystal phase. From the full width at half maximum (FWHM) of the most intense diffraction peak at $2\theta = 23.6^o$ of $LiTaO_3$ and $2\theta = 30^o$ of $KNbO_3$, the average crystallite size (diameter, d) is calculated by using the Scherrer's formula[27]

$$d = 0.9\lambda / \beta \cos\theta \qquad (1)$$

where λ is the wavelength of X-ray radiation (CuK_α = 1.5406Å), β is the full width at half maximum (FWHM) of the peak at 2θ. The average $LiTaO_3$ crystallite size increases with heat-

treatment duration and found to vary from 35 to 60 nm. For $KNbO_3$ crystallite containing nano glass-ceramics the crystallite size is estimated to be around 15 nm.

3.2 TEM Image Analysis

The morphology and distribution of $LiTaO_3$ and $KNbO_3$ crystallite containing nano glass-ceramics have been examined by TEM image analysis. The TEM bright field images and their corresponding selected area electron diffraction (SAED) patterns of the heat-treated (at 680^oC for 10 h) $LiTaO_3$ nano glass-ceramic and heat-treated (800^oC for 10 h) $KNbO_3$ nano glass-ceramic samples are shown in Figs. 5(a) and (b) respectively. From these images, it is observed that many irregular size and shaped $LiTaO_3$ and nearly spherical $KNbO_3$ crystallites precipitated homogeneously and remained dispersed in the residual glass matrix. The crystallite size from TEM image of Fig. 5(a) is found to be around 15-30 nm and Fig. 5(b) to be around 12 nm. The presence of fine spherical rings around the central bright region in SAED pattern discloses the existence of $LiTaO_3$ and $KNbO_3$ crystallites in the glassy matrix.

3.3 SHG Analysis

Some basic principles of nonlinear optics are discussed as follows. For a more comprehensive article, the reader is referred to other literature on nonlinear optics.[28-32] A general introduction to (linear) crystal optics can be found in standard textbooks.[33-35] The NLO processes originate from the response of a nonlinear dielectric medium to an oscillating electric field. For an applied low amplitude oscillating field on the crystal structure and its electron distribution the induced oscillation of charges in the structure results in the radiation of an electromagnetic field with a frequency equal to the applied field oscillation. If, however, a harmonic oscillation with

sufficiently high amplitude is applied, then radiation that is described by a combination of the induced frequency and its harmonics is produced. Therefore, NLO processes in optical media, caused by intense electromagnetic radiation fields, generate new frequencies of light. With respect to the electromagnetic field the processes can either be energy conserving such as harmonic generation or energy consuming such as stimulated Raman or Brillouin scattering. In harmonic generation, a single harmonic (frequency doubling, tripling, etc.) of a given fundamental frequency is generated by the nonlinear response of the material. The induced dielectric polarization P depends on the applied field E and can be expressed in a series of powers of E, according to Eq. 2, where $\chi^{(1)}$ is the linear dielectric susceptibility known from linear optics, and $\chi^{(2)}$, $\chi^{(3)}$, etc. are the nonlinear dielectric susceptibilities of second, third, etc. order, respectively.

$$P(E) = \varepsilon_o(\chi^{(1)}E + \chi^{(2)}E^2 + \chi^{(3)}E^3 + - - -) \qquad (2)$$

Unfortunately, not all materials are suitable for NLO applications. Nonlinear second-order susceptibility only occurs in crystals without a center of symmetry, in centric crystals or amorphous materials (e.g., glass) it is zero. In the case of SHG ($\omega_1 = \omega_2$, $\omega_3 = 2\omega_1$, $\omega_{n=1,\,2,\,3}$ are the frequency terms of $\chi^{(n)}$) a SHG tensor d_{ijk} is commonly used in the literature, which is defined as $d_{ijk} = \chi_{ijk}/2$. In other way, in this process two identical photons from a single pump beam are added, resulting in a photon having twice the frequency. The generation of second-harmonic waves from the incident wave of frequency ω_1 is a two-step process. First, a polarization wave at the second harmonic frequency $2\omega_1$ is produced. The next step is the transfer of energy from the polarization wave to an electromagnetic wave at frequency $2\omega_1$. The phase velocity of the fundamental as well as the second harmonic depends upon the refractive index of the medium at respective wavelengths.

The variation of SHG output power (nJ) with time period in LTSA glass and LT glass-ceramics has been shown in Fig. 6(a)-(d). It is seen from the Fig. 6(a) that the precursor LTSA glass does not exhibit any SHG output. This is due to inversion symmetry of the precursor glass. For a constant heat-treatment time (10 h), the SHG output power increase from 1.08 to 1.875 nJ when the temperature is increased from 680^{o}C to 850^{o}C. This is attributed due to the formation of ferroelectric (non-centrosymmetric) $LiTaO_3$ crystals in the glassy matrix. Moreover, the increase in SHG output power with subsequent increase of heat-treatment temperature is due to the increase of $LiTaO_3$ crystallites content and their sizes in the glassy matrix. The variation of SHG output power from 1 x 1 x 1 and 3 x 1 x 1 cm^3 bulk samples with time period has been presented Fig. 7(a) and (b). With increase in length of the sample, the output SHG power is also increased from 1.08 nJ to 1.126 nJ and this may be due the availability of relatively more number $LiTaO_3$ ferroelectric crystallites in glass-ceramics. The variation of SHG output power with angle of rotation (0-32.5^{o}) is shown in Fig. 8. With variation of rotation angle, the nano glass-ceramics exhibit maximum SHG output (14 nJ) at an angle of 8^{o}. This phenomenon is explained on the basis of reorientation of ferroelectric domains under the applied electric field. A similar observation and explanation were reported by Borrelli et al.[36,37]

The SHG output power (nJ) of KNS glass and KN glass-ceramics heat-treated at 800^{o}C for 10 h is shown in Fig. 9(a)-(b). It is seen from the Fig. 9(a) that the precursor glass does not exhibit any SHG output. This phenomenon once again explained on the basis of inversion symmetry of the precursor glass. With heat-treatment of the precursor glass at 800^{o}C for 10 h duration, the SHG output power increase to 39.74 nJ. This is attributed due to the formation of ferroelectric (non-centrosymmetric) $KNbO_3$ crystals in the glassy matrix. The variation of SHG output power of the glass-ceramic composite material with angle of rotation (0-32.5^{o}) is shown

in Fig. 10. With variation of rotation angle, the nano glass-ceramics exhibit maximum SHG output (62.4 nJ) at an angle of 4^{o}. It is also happened due to reorientation of ferroelectric domains under the applied electric field.[36,37]

4. Conclusions

We have prepared LT and KN nano glass-ceramics by controlled crystallization of the corresponding precursor glasses. X-ray diffraction (XRD) and transmission electron microscopic (TEM) analyses confirm the formation of $LiTaO_3$ crystals in LTSA glass system and $KNbO_3$ crystals in KNS glass system. The crystallite sizes of the LT are in the range 35-60 nm and KN is about 15 nm. We have demonstrated the second harmonic generation (SHG) in the aforementioned two bulk nano glass-ceramics. It is attributed to the formation of non-centrosymmetric ferroelectric $LiTaO_3$ and $KNbO_3$ nano crystals. It is also observed that with increase of ferroelectric phases ($LiTaO_3$ and $KNbO_3$) and its sizes, the SHG output powers have also increased and found to vary in the range 1.08 to 39.74 nJ. The variation of SHG output powers with the changes of rotation angle for LT and KN nano glass-ceramics have been studied and the maximum values of SHG output are 14 nJ and 62.4 nJ respectively.

Acknowledgements

This research work was supported by BRNS/DAE under the sanction No. 2007/34/05-BRNS. The authors gratefully thank Director of the institute for his keen interest and kind permission to publish this paper. The technical supports provided by the infrastructural facility (X-ray and Electron Microscopy Divisions) of this institute are also thankfully acknowledged.

References

1. T. H. Maiman, Stimulated optical radiation in ruby, *Nature* **187** (1960) 493-494.
2. P.A. Franken, A. E. Hill, C.W. Peters and G. Weinreich, Generation of optical harmonics, *Phys. Rev. Lett.* **7** (1961) 118-119.
3. P.F. Bordui and M. M. Fejer, Inorganic crystals for nonlinear optical frequency conversion, *Annu. Rev. Mater. Sci.* **23** (1993) 321-379.
4. V. G. Dmitriev, G. G. Gurzadyan and D. N. Nikogosyan, in *Handbook of Nonlinear Optical Crystals 2nd Ed.*, Ed. by A.E. Siegman, (Springer –Verlag, 1997), p. 301.
5. K. S. Abedin, T. Tsuritani, M. Sato and H. Ito, Integrated intracavity quasi-phase-matched second harmonic generation based on periodically poled Nd:$LiTaO_3$, *Appl. Phys. Lett.* **70** (1997) 10-12.
6. S. Zhu, Y. Zhu, Z. Yang, Z. Yang, H. Wang, Z. Zhang, J. Hong, C. Ge and N. Ming, Second-harmonic generation of blue light in bulk periodically poled $LiTaO_3$, *Appl. Phys. Lett.* **67** (1995) 320-322.
7. D. Xue and S. Zhang, Comparison of non-linear optical susceptibilities of $KNbO_3$ and $LiNbO_3$, *J. Phys. Chem. Solids* **58** *(*1997) 1399-1402.
8. K.J. Lee, C.S. Yoon and F. Rotermund, Phase Matching Characteristics of Second-Harmonic Generation in Periodic 90°-Domain Structures of $KNbO_3$, *Jpn. J. Appl. Phys.* **46** (2007) 7317-7320.
9. I. Sokólska, W. Ryba-Romanowski, S. Gołab, M. Baba, M. Świrkowicz and T. Łukasiewicz, Spectroscopy of $LiTaO_3:Tm^{3+}$ crystals, *J. Phys. Chem. Solids* **61** (2000) 1573-1581.
10. Y. Uematsu, Nonlinear optical properties of $KNbO_3$ single crystal in the orthorhombic phase, *Jpn. J. Appl. Phys.* **13** (1974) 1362-1368.

11. S.C. Abrahams and J.L. Bernstein, Ferroelectric lithium tantalate-1. single crystal X-ray diffraction study at 24°C, *J. Phys. Chem. Solids* **28** (1967) 1685-1692.

12. S.C. Abrahams, Walter C. Hamilton and A. Sequeira, Ferroelectric lithium tantalate-2. Single crystal neutron diffraction study at 24°C, *J. Phys. Chem. Solids* **28** (1967) 1693-1698.

13. M. Wiegel, M. H. J. Emond, E. R. Stobbe and G. Blasse, Luminescence of alkali tantalates and niobates, *J. Phys. Chem. Solids* **55** (1994) 773-778.

14. A. Winiarski, T. Neumann, B. Mayer, G. Borstel and M. Neumann, XPS study of $KTaO_3$, $KTa_{0.69}Nb_{0.31}O_3$, and $KNbO_3$ single crystals, *phys. status solidi b* **183** (1994) 475-480.

15. W. Nie, Optical nonlinearity: phenomena, applications, and materials, *Adv. Mater.* **5** (1993) 520-545.

16. E. Fargin, A. Berthereau, T. Cardinal, G. Le Flem, L. Ducasse, L. Canioni, P. Segonds, L. Sarger and A. Ducasse, Optical non-linearity in oxide glasses, *J. Non-Cryst. Solids* **203** (1996) 96-101.

17. M. Miyata, H. Nasu, A. Mito, K. Kurachi, J. Matsuoka and K. Kamiya, Second-harmonic generation from electrically poled niobium alkali silicate glasses, *Jpn. J. Appl. Phys. Part-2* **34** (1995) L1455-L1457.

18. H. Nasu, K. Kurachi, A. Mito, H. Okamoto, J. Matsuoka and K. Kamiya, Second harmonic generation from an electrically polarized TiO_2-containing silicate glass, *J. Non-Cryst. Solids* **181** (1995) 83-86.

19. K. Tanaka, K. Kashima, K. Hirao, N. Soga, A. Mito and H. Nasu, Second harmonic generation in electrically poled Li_2O-Nb_2O_5-TeO_2 glasses, *J. Non-Cryst. Solids* **185** (1995) 123-126.

20. V.I. Kopp, I.V. Mochalov, N.V. Nikonorov and I.F. Salahetdinov, Photoinduced chi recording in two- and multicomponent lead-silicate glasses for optical waveguides, *Proc. SPIE—Int. Soc. Opt. Eng.* **2150** (1994) 314-318.

21. V. Nazabal, E. Fargin, J. J. Videau, G. Le Flem, A. Le, Calvez, S. Montant, E. Freysz, A. Ducasse and M. Couzi, Second-harmonic generation of electrically poled borophosphate glasses: effects of introducing niobium or sodium oxides, *J. Solid State Chem.* **133** (1997) 529-535.

22. K. Tanaka, Optical nonlinearity in photonic glasses, *J. Mater. Sci.: Mater. Electron.* **16** (2005) 633-643.

23. L.R.P. Kassab, R. Miedzinski, I.V. Kityk, J. Ebothe, D.M. da Dilva and A.H. Reshak, Electron beam induced second-harmonic generation in Er^{3+} doped PbO-GeO_2 glasses containing silver nanoparticles, *J. Mater. Sci.: Mater. Electron.* **20** (2009) 87-91.

24. A. Tarafder, K. Annapurna, R.S. Chaliha, V.S. Tiwari, P.K. Gupta and B. Karmakar, Processing and properties of Eu^{3+}:$LiTaO_3$ transparent glass-ceramic nanocomposites, *J. Am. Ceram. Soc.* **92** (2009) 1934-1339.

25. R.S. Chaliha, K. Annapurna, A. Tarafder, V.S. Tiwari, P.K. Gupta and B. Karmakar, Luminescence and dielectric properties of nano-structured Eu^{3+}:K_2O-Nb_2O_5-SiO_2 glass-ceramics, *Solid. State. Sci.* **11** (2009) 1325-1332.

26. J. S. de Andrade, A. G. Pinheiro, I. F. Vasconcelos, M. A. B. de Araújo, M. A. Valente and A. S. B. Sombra, Structural studies of $KNbO_3$ in niobate glass-ceramics, *J. Phys. Chem. Solids* **61** (2000) 899-906.

27. B. D. Cullity, *Elements of X-Ray Diffraction 2nd Ed.* (Addison-Wesley Publishing Co., London, 1978), p.101.

28. A. Yariv and P. Yeh, *Optical Waves in Crystals* (Wiley, New York, 1984).

29. G. C. Baldwin, *Nonlinear Optics* (Plenum, New York, 1969).

30. N. Bloembergen, *Nonlinear Optics* (Benjamin, New York, 1965).

31. F. Zernicke and J. E. Midwinter, *Applied Nonlinear Optics* (Wiley, New York, 1973).

32. Y. R. Shen, *The Principles of Nonlinear Optics* (Wiley, New York, 1984).

33. M. Born and E. Wolf, *Principles of Optics* (Pergamon, London, 1959).

34. N. F. Nye, *Physical Properties of Crystals* (Clarendon, Oxford, 1960).

35. G. N. Ramachandran, S. Ramaseshan, in *Handbuch der Physik*, Vol. 15/1, Ed. by S. Flügge, (Springer, Berlin, 1961), p.1.

36. N. F. Borrelli, Electro-optic effect in transparent niobate glass-ceramic systems, *J. Appl. Phys.* **38** (1967) 4243-4247.

37. N. F. Borrelli and M. M. Layton, Electrooptic properties of transparent ferroelectric glass-ceramic systems, *IEEE Trans. Electron Dev.* **16** (1969) 511-514.

FIGURE CAPTIONS

Fig. 1. Schematic diagram of experimental arrangement for measuring bulk SHG efficiency.

Fig. 2. Photograph of (a) LT precursor bulk glass (extreme left, one number) and nano glass-ceramics (right, three numbers) and (b) KN precursor bulk glass (extreme left, one number) and nano glass-ceramics (right, three numbers) used to measure SHG efficiency.

Fig. 3. XRD patterns of precursor LTSA glass and LT nano glass-ceramics obtained after heat-treatment at 680, 750 and 850^{o}C 10 h.

Fig. 4. XRD patterns of precursor KNS glass and KN nano glass-ceramics obtained after heat-treatment at 800^{o}C for 10 h.

Fig. 5. (a) TEM images and SAEDs (Inset) of nano glass-ceramic samples (a) LT heat-treated at 680^{o}C for 10 h and (b) KN heat-treated at 800^{o}C for 10 h.

Fig. 6. Variation of SHG output power (nJ) with time period of precursor LTSA glass, 680, 750, and 850^{o}C heat-treated for 10 h LT nano glass-ceramic samples.

Fig. 7. Variation of SHG output power with time period of 1 x 1 x 1 and 3 x 1 x 1 cm^3 LT nano glass-ceramic samples heat-treated at 680^{o}C for 10 h.

Fig. 8. Variation of SHG output power with angle of rotation (degree) of 3 x 1 x 1 cm^3 LT nano glass-ceramics sample heat-treated at 680^{o}C for 10 h.

Fig. 9. Variation of SHG output power (nJ) with time period of precursor KNS glass and 800^{o}C heat-treated for 10 h KN nano glass-ceramic samples.

Fig. 10. Variation of SHG output power with angle of rotation (degree) of KN nano glass-ceramic sample heat-treated at 800^{o}C for 10 h.

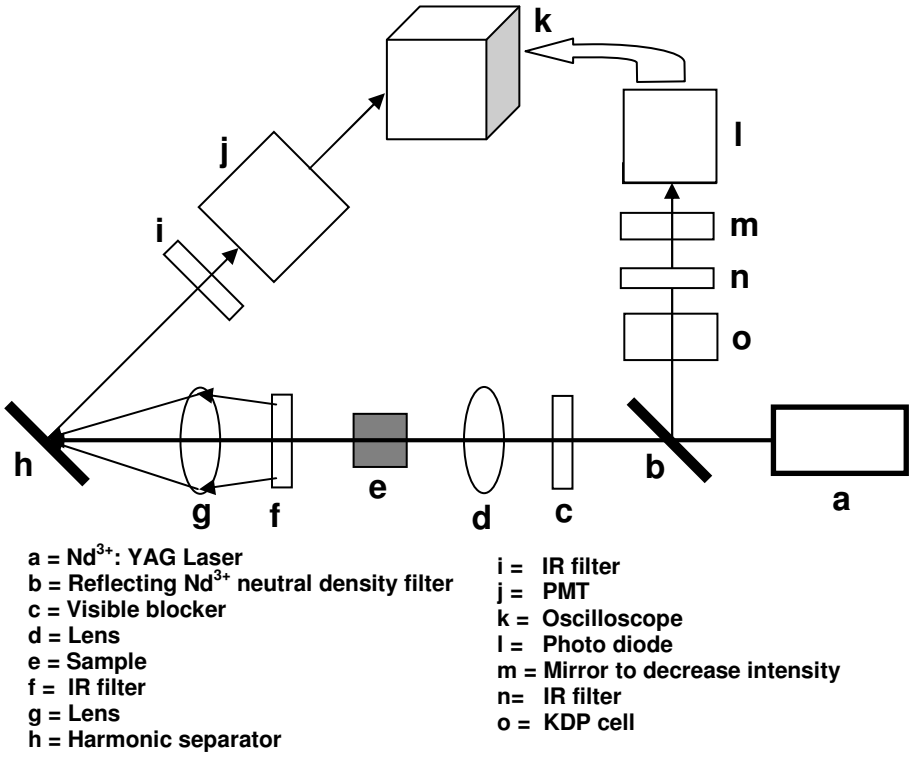

Fig. 1. Schematic diagram of experimental arrangement for measuring bulk SHG efficiency.

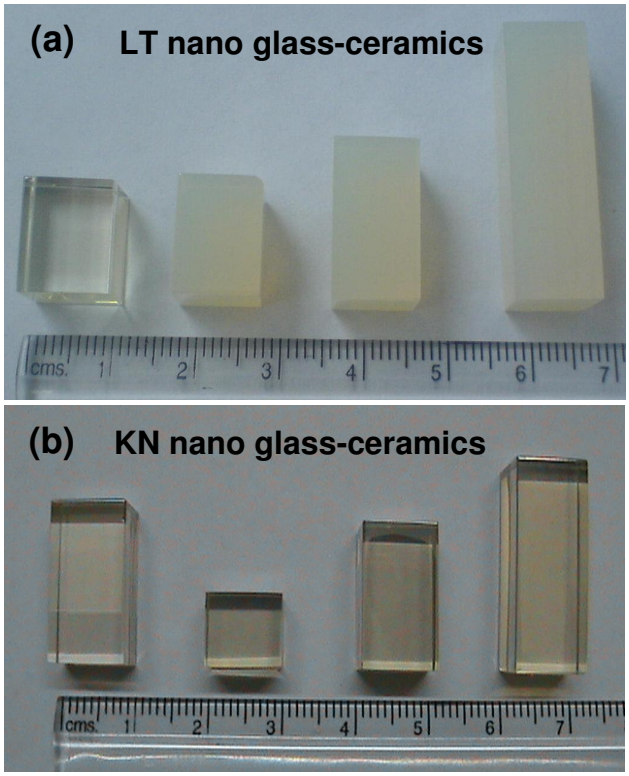

Fig. 2. Photograph of (a) LT precursor bulk glass (extreme left, one number) and nano glass-ceramics (right, three numbers) and (b) KN precursor bulk glass (extreme left, one number) and nano glass-ceramics (right, three numbers) used to measure SHG efficiency.

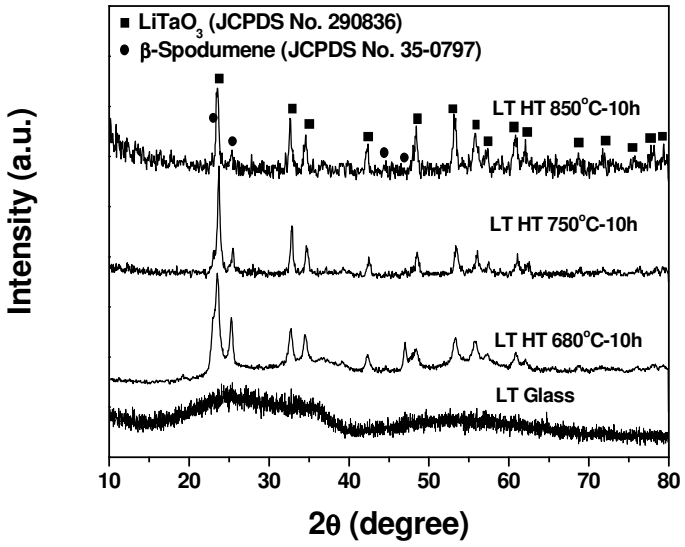

Fig. 3. XRD patterns of precursor LTSA glass and LT nano glass-ceramics obtained after heat-treatment at 680, 750 and 850°C 10 h.

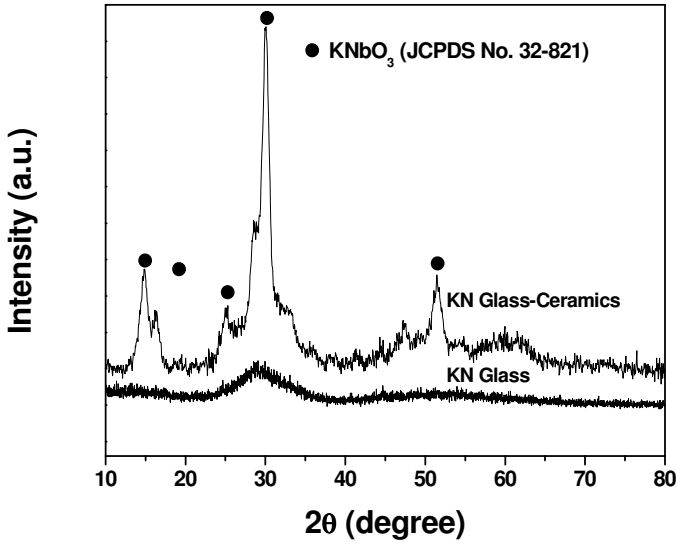

Fig. 4. XRD patterns of precursor KNS glass and KN nano glass-ceramics obtained after heat-treatment at 800^{o}C for 10 h.

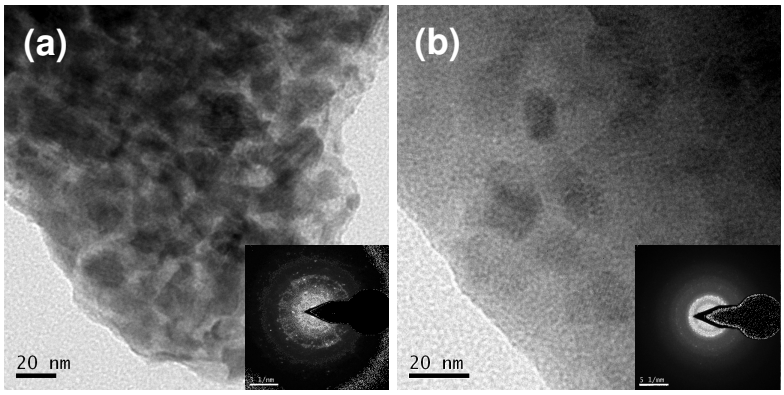

Fig. 5. (a) TEM images and SAEDs (Inset) of nano glass-ceramic samples (a) LT heat-treated at 680^{o}C for 10 h and (b) KN heat-treated at 800^{o}C for 10 h.

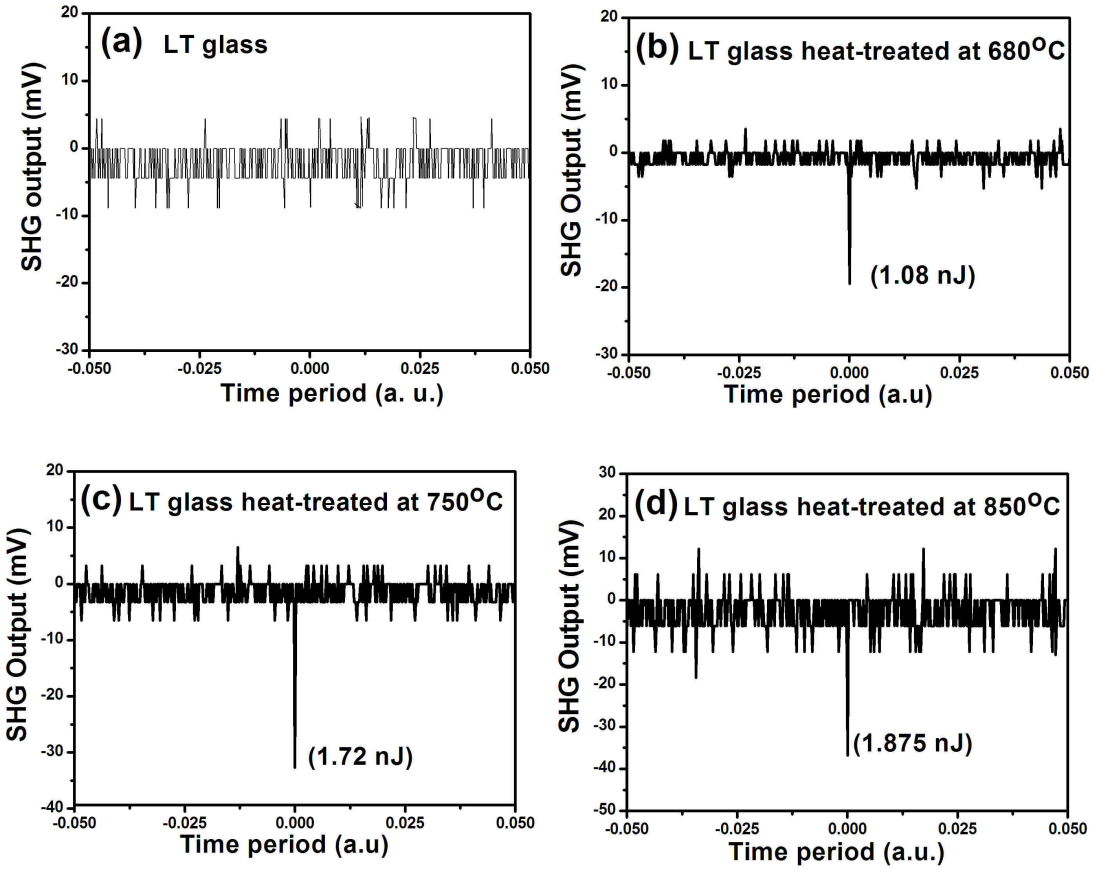

Fig. 6. Variation of SHG output power (nJ) with time period of precursor LTSA glass, 680, 750, and 850^{o}C heat-treated for 10 h LT nano glass-ceramic samples.

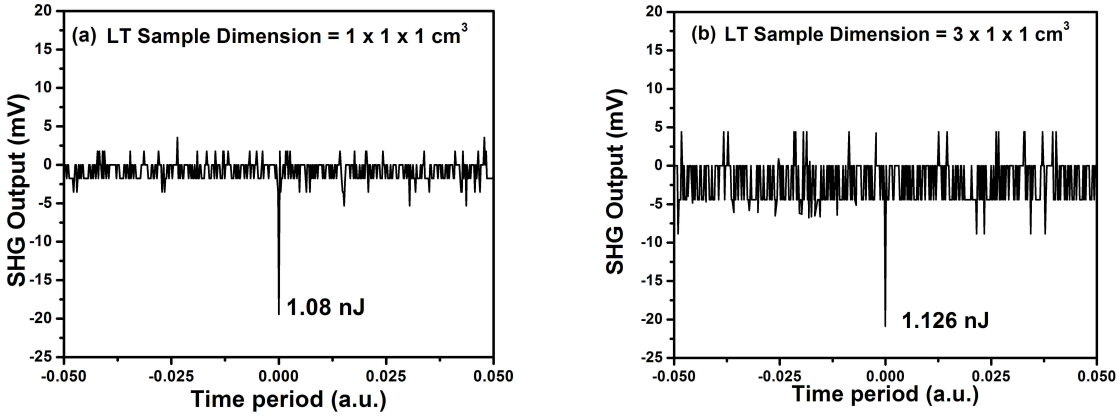

Fig. 7. Variation of SHG output power with time period of 1 x 1 x 1 and 3 x 1 x 1 cm^3 LT nano glass-ceramic samples heat-treated at 680^oC for 10 h.

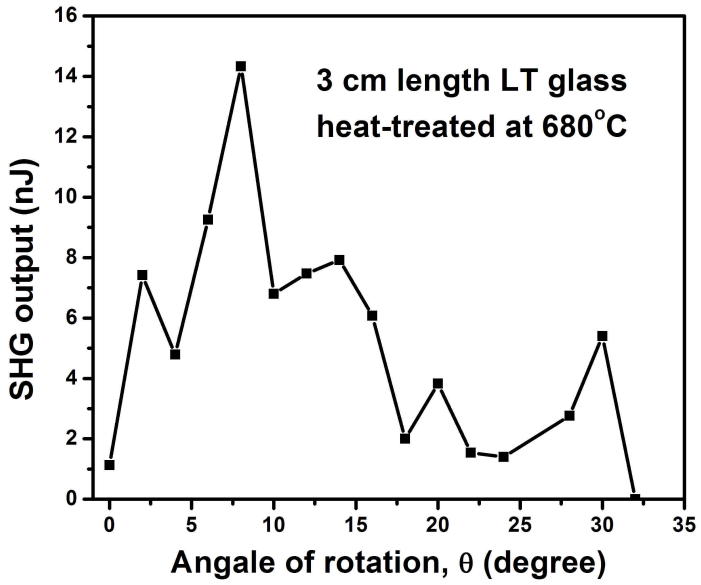

Fig. 8. Variation of SHG output power with angle of rotation (degree) of 3 x 1 x 1 cm^3 LT nano glass-ceramics sample heat-treated at 680°C for 10 h.

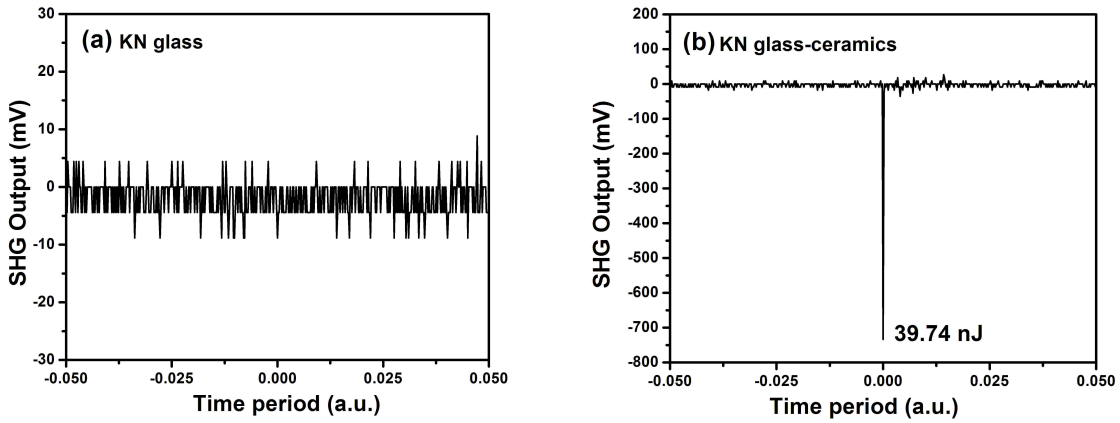

Fig. 9. Variation of SHG output power (nJ) with time period of precursor KNS glass and 800^{o}C heat-treated for 10 h KN nano glass-ceramic samples.

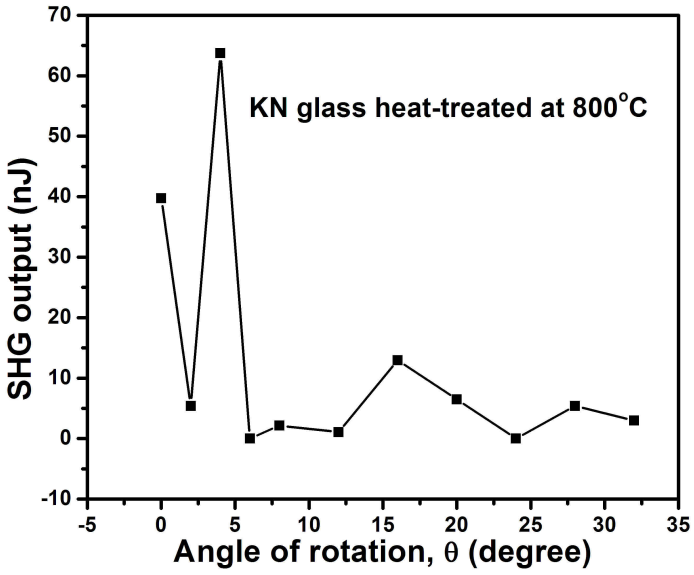

Fig. 10. Variation of SHG output power with angle of rotation (degree) of KN nano glass-ceramic sample heat-treated at 800°C for 10 h.